Myostatin dysfunction is associated with reduction in overload induced hypertrophy of soleus muscle in mice

Minderis, P; Kilikevicius, A; Baltusnikas, J; Alhindi, Y; Venckunas, T; Bunger, L; Lionikas, A; Ratkevicius, A

Published in:
Scandinavian Journal of Medicine Science in Sports

DOI:
10.1111/sms.12532

Print publication: 01/01/2015

Document Version
Peer reviewed version

SCANDINAVIAN JOURNAL OF MEDICINE & SCIENCE IN SPORTS

Myostatin dysfunction is associated with reduction in overload induced hypertrophy of soleus muscle in mice

Journal:	*Scandinavian Journal of Medicine and Science in Sports*
Manuscript ID:	Draft
Manuscript Type:	Original Article
Date Submitted by the Author:	n/a
Complete List of Authors:	Minderis, Petras; Lithuanian Sports University, Institute of Sport Science and Innovations Kilikevicius, Audrius; Lithuanian Sports University, Institute of Sport Science and Innovations Baltusnikas, Juozas; Lithuanian Sports University, Institute of Sport Science and Innovations Alhindi, Yosra; University of Aberdeen, School of Medical Sciences Venckunas, Tomas; Lithuanian Sports University, Institute of Sport Science and Innovations Bunger, Lutz; Scotland's Rural College (SRUC), Animal Breeding and Genetics, Animal and Veterinary Sciences group Lionikas, Arimantas; University of Aberdeen, School of Medical Sciences Ratkevicius, Aivaras; University of Aberdeen, School of Medical Sciences
Keywords:	Skeletal muscle, muscle hypertrophy, contractile properties, p70S6K, high resistance exercise

Myostatin dysfunction is associated with reduction in overload induced hypertrophy of soleus muscle in mice

P. Minderis[1], A. Kilikevicius[1], J. Baltusnikas[1], Y. Alhindi[3], T. Venckunas[1], L. Bunger[2], A. Lionikas[1,3], A. Ratkevicius[1,3]

[1]Institute of Sport Science and Innovations, Lithuanian Sports University, Kaunas, Lithuania, [2]Animal Breeding and Genetics, Animal and Veterinary Sciences group, Scotland's Rural College (SRUC), Edinburgh, UK, [3]School of Medical Sciences, College of Life Sciences and Medicine, University of Aberdeen, Aberdeen, Scotland, UK

Running title: Myostatin in resistance exercise

Corresponding author:

Dr. Aivaras Ratkevicius

School of Medical Sciences, College of Life Sciences and Medicine, Applied Health Science Building, University of Aberdeen, Foresterhill, Aberdeen, AB25 2ZD, Scotland, U.K.

Tel: +44 (0)1224 38023

E mail: a.ratkevicius@abdn.ac.uk

Abstract

The aim of the study was to investigate if myostatin dysfunction would promote the gain in muscle mass and peak isometric force (P_0) of soleus muscle (SOL) in response to functional overloading (FO) after ablation of the gastrocnemius muscle. Fifteen male Berlin high (BEH) mice homozygous for the compact mutation causing dysfunction of myostatin and seventeen mice with the corresponding wild type allele (BEH+/+) were subjected to FO of SOL for 28 days at the age of 14 weeks. Compared to BEH+/+ mice, SOL of BEH was heavier (mean ± SD, 13.5 ± 1.5 vs 21.4 ± 1.8 mg, respectively, $P < 0.001$). After FO, SOL mass increased relatively more in BEH+/+ than BEH strain (34.9 ± 11.5 vs 17.7 ± 11.9 %, respectively, $P < 0.01$). P_0 fell ($P < 0.01$) only in BEH strain which also showed an increase ($P < 0.01$) in optimal muscle length. Specific P_0 became even more depressed in BEH compared to BEH+/+ strain (8.4 ± 1.4 *versus* 10.8 ± 1.3 N/g, respectively, $P < 0.001$). Phosphorylation p70 S6 kinase did not differ between the strains. In summary, myostatin dysfunction impairs adaptation of SOL muscle to high functional demands.

Key words: Skeletal muscle, muscle hypertrophy, contractile properties, p70S6K, high resistance exercise

Introduction

Skeletal muscle mass is an important factor contributing to health and wellbeing (Wolfe, 2006), and there is a significant interest in ways to promote muscle mass and strength in humans of different ages and health status (Stewart *et al.*, 2013). Much of the debate has recently focused around myostatin (Smith and Lin, 2013).

Myostatin, a member of the TGF-β super family, is a potent inhibitor of muscle growth in mammals (McPherron *et al.*, 1997). Mouse models with impaired function of myostatin show an increase in skeletal muscle mass as a result of muscle fiber hypertrophy and hyperplasia (McPherron *et al.*, 1997). Myostatin dysfunction is associated with enhanced mammalian target of rapamycin signalling which induces muscle growth in response to functional overloading (Lipina *et al.*, 2010, Goodman *et al.*, 2011). Phosphorylation of p70 S6 kinase (p70S6K) which is associated with mTOR activation correlates with the increase in muscle mass after resistance training in mice (Baar and Esser, 1999). These observations suggested that inhibition of myostatin could preserve and restore contractile tissue in various muscle wasting conditions. Indeed, intraperitoneal injections of myostatin blocking antibodies induce an increase in muscle mass of dystrophic mouse model (Bogdanovich *et al.*, 2002). There is also evidence that acute resistance exercise decreases myostatin signaling through the activation of the TGFβ inhibitor Notch (MacKenzie *et al.*, 2013). However, effectiveness of myostatin inhibition as a treatment against loss of muscle function is unclear. Mice with dysfunctional myostatin show reduced specific force of the extensor digitorum longus (EDL) muscle (Mendias *et al.*, 2006, Amthor *et al.*, 2007). We have observed a reduction in specific force of Xenopus muscle fibers treated with SB431542 that acts to inhibit myostatin signaling through Smad transcriptional factors (Watt *et al.*, 2010). Furthermore, we did not detect any differences in plasma myostatin levels between young men and older men showing significant loss of muscle mass and strength (Ratkevicius *et al.*, 2011).

There are also large knowledge gaps about the role of myostatin in adaptation of skeletal muscle to exercise. Myostatin dysfunction leads to the shift towards faster contracting myosin isoforms which is the likely mechanism underlying the reduced endurance capacity of myostatin deficient mice (Matsakas *et al.*, 2010). Yet decreased or abolished myostatin signaling might be advantageous for adaptations to resistance training since type II fibres show greater enlargement in the cross sectional area compared to type 1 fibres (Verdijk *et al.*, 2009). However, to the best of our knowledge, this hypothesis has not been tested.

Mouse soleus muscle (SOL) consists primarily of type 1 and type 2A fibers with some (~10%) type 2X fibres and thus differs from the other appendicular muscles in rodents dominated by type 2B, 2X and 2A fibers (Amthor *et al.*, 2007, Bloemberg and Quadrilatero, 2012). This similarity to human muscles (Bloemberg and Quadrilatero, 2012) makes mouse SOL a prudent model for examining the role of myostatin in the adaptive response to resistance training. Functional overloading (FO) after synergists ablation has been widely used to study muscle hypertrophy in rodents (Lowe and Alway, 2002). The main aim of our study was to test the hypothesis that myostatin dysfunction would increase the gain in mass and isometric force of SOL after ablation of the gastrocnemius muscle. We studied Berlin High mice which carried either a mutant myostatin alleles known as compact (BEH) or wild type myostatin alleles, BEH+/+ (Amthor *et al.*, 2007, Lionikas *et al.*, 2013).

Materials and methods

Animals and study design

All procedures involving mice were approved by the Lithuanian State Food and Veterinary Service (Nr. 0223). Mice were housed in standard cages, one to three mice per cage at a temperature of 22-24 ºC and 40-60 % humidity as in our previous studies (Ratkevicius *et al.*, 2010, Kilikevicius *et al.*, 2012). Animals were fed standard chow diet and received tap water ad libitum. BEH+/+ animals were generated by crossing animals from BEH and Berlin Low

(BEL) strains and then repeatedly backcrossing the offspring to BEH using marker assisted selection for the wild type myostatin (Amthor *et al.*, 2007, Lionikas *et al.*, 2013, Bunger *et al.*, 2004). We used males of the 17th or higher generation of backcrossing, homozygous for the wild type allele of myostatin (BEH+/+) and male BEH mice homozygous for the compact allele.

Initially, citrate synthase (CS) activity, a mitochondrial marker (Jacobs *et al.*, 2013), was studied in the gastrocnemius (GAS), plantaris (PLAN) and Sol muscles of six BEH mice and six BEH+/+ mice at the age of ~14 weeks . Then fifteen BEH mice and eighteen BEH+/+ mice were subjected to the functional overload of Sol for 28 days starting at the age of 14 weeks. These animals were anesthetized with an intraperitoneal injection of ketamine (100 mg/kg) and xylazine (10 mg/kg), and the gastrocnemius muscle (GAS) was surgically removed from a randomly selected leg using similar methods as described earlier (Hamilton *et al.*, 2010). Mice were given buprenorphine after surgery for pain relief and were monitored on a daily basis. The contralateral SOL of these mice served as internal control in analysis of muscle mass, p70S6K phosphorylation and cytochrome c levels. Twelve BEH+/+ and twelve BEH mice were not subjected to any interventions and used as age matched independent controls in the analysis of muscle properties.

Assessment of muscle properties

Similar procedures as in our previous studies were used (Baltusnikas *et al.*, 2015). Mice were euthanized at 18 weeks of age. Sutures were attached to the proximal and distal tendons of Sol for measurements of contractile properties. The muscle was then excised and fixed between two platinum plate electrodes in 50 ml Radnotti tissue bath filled with the Tyrode solution (121 mM NaCl, 5 mM KCl, 0.5 mM $MgCl_2$, 1.8 mM $CaCl_2$, 0.4 mM NaH_2PO_4, 0.1 mM NaEDTA, 24 mM $NaHCO_3$, 5.5 mM glucose, pH adjusted to 7.4 when bubbled with 95 % O_2 and 5 % CO_2. The distal tendon of the muscle was attached to a hook and the proximal

end was tied directly to the lever of muscle test system (1200A-LR Muscle Test System, Aurora Scientific Inc., Aurora, Canada). The muscle was then left to equilibrate in the solution for 10 min. In the meantime the contralateral soleus muscle was dissected and placed in the Tyroid solution bubbled with 95 % O_2 and 5 % CO_2. All experiments were carried out at room temperature of ~23 °C. The length of the fixed muscle was increased in steps every 30 s just after delivery of electrical pulse to evoke a twitch contraction. This procedure was continued until twitch force did not increase with the increase in muscle length. The muscle was then photographed with the length scale in the background to assess muscle length with a precision of 0.1 mm. Muscles were kept at this optimal length during the assessment of contractile properties. Firstly, single twitches were generated and peak twitch force was measured. The twitch contraction time was assessed as the time from the beginning of the contraction to the peak of twitch force. Twitch half relaxation time was measured as the time taken for force to decline from peak to 50 % of peak value. Afterwards, the muscle was subjected to 900 ms trains of stimuli at 20, 50, 80, 100 and 150 Hz for assessment of peak isometric force. Assessment of contractile properties was completed by eccentric exercise consisting of 20 repeated eccentric contractions performed every 10 s. Each eccentric contraction was induced by 1100 ms stimulation at a frequency needed to generate peak force (80 or 100 Hz). During the last 200 ms of this stimulation a ramp stretch was imposed followed by a 200 ms gradual return of the muscle to the initial length without any stimulation. The amplitude of the stretch was 30 % of muscle fibre or 2.5 fiber lengths per second assuming fibre length to muscle length ratio of 0.7 (Brooks and Faulkner, 1988). Peak isometric force was measured during the initial 900 ms of contraction. Then these muscles were incubated in 2 ml of Tyrode solution for 2 h at room temperature. 250 µl of Tyrode solution was sampled for assessment of CK activity using biochemical analyser (Spotchem™ EZ SP-4430, Menarini Diagnostics, UK) with the reagent strips (Arkray Factory, Inc., Shiga,

Japan). Following all measurements both control and experimental muscle were freed from tendons, blotted and weighed (Kern, ABS 80-4, Germany). Afterwards, muscles were dried for 48 h at a temperature of 40 °C and the weighed again for estimation of dry muscle weight.

Citrate synthase (CS) assay

CS activity measurements were performed as previously described (Ratkevicius *et al.*, 2010). Mice were euthanized at 14 weeks of age. Then muscles were excised, snap frozen in isopentane pre-cooled by liquid nitrogen and stored at -80 °C. Muscle samples were then homogenised in ice cold lysis buffer (50 mM Tris-HCl, 1 mM EDTA, 1 mM EGTA, 1% (vol/vol) Triton X-100, 0.1 % (vol/vol) 2-mercaptoethanol, pH was adjusted to 7.5) supplemented with protease inhibitor cocktail, 10 mM β-glycerophosphate, 50 mM NaF and 0.5 mM Na_3VO_4. Two or three Sol and Plan muscles and approximately half of Gas muscle (~60 mg) were used in the corresponding muscle sample. The homogenates were frozen in liquid nitrogen, then thawed and shaken at 4 °C for 60 min followed by centrifugation at 13,000 g for 10 min. The supernatants were taken and the protein concentration was determined using the Bradford Assay (Bio-rad, Hertfordshire, UK) and GENESYS 10 Bio UV-Vis Spectrophotometer (Thermo Fisher Scientific Inc., Waltham, MA, USA). The same spectrophotometer was used for assessment of CS activity. The reaction reagent consisted of 100 mM triethanolamine-HCl, DTNB (100 μM), 0.25 % Triton-X (vol/vol), 0.5 mM oxaloacetate, 0.31 mM acetyl CoA with pH adjusted to 8.0. Ten μl of muscle homogenate was added to start the reaction in 1000 μl. The molar extinction coefficient of 13,600 $M^{-1} \cdot cm^{-1}$ was used to assess the maximum CS activity at 412 nm during the first 2 min of the reaction. The assays were carried out at room temperature (~21 °C). CS from porcine heart was used as a standard (C3260-200UN, Sigma-Aldrich, UK) for assay calibration.

Western blotting

Muscle homogenates were prepared as described for CS assays (Ratkevicius *et al.*, 2010). Then samples containing 50 μg protein were loaded on 10% polyacrylamide gel, separated using SDS-PAGE electrophoresis and then transferred to polyvinylidene fluoride (PVDF) membrane. Then membranes were washed with Tris buffered saline (TBS) containing 0.1 % (vol/vol) Tween-20 (TBS-T buffer) before two hour incubation in the blocking buffer (5 % (wt/vol) non-fat milk in TBS-T buffer). The membranes were incubated for 18 h at 4 °C with a primary antibody at 1:1000 dilution (vol / vol) TBS-T buffer supplemented with 5% bovine serum albumin. All antibodies were from Cell Signaling Technology (Danvers, MA, USA). The following primary antibodies were used; Phospho-p70 S6 Kinase (Thr389) or P-p70S6K (#9205), p70 S6 Kinase or p70S6K (#9202), cytochrome c or Cyt C (#4272) and β-Actin (#4967). After incubation with a primary antibody, membranes were washed in TBS-T buffer and exposed for 2 h to HRP-conjugated secondary antibody (#7071) at 1:2000 dilution in the blocking buffer. The imaging of blots was performed using ECL reagent (Amersham Biosciences, Buckinghamshire, UK) and Fluor-SMax Imager (Bio-rad, Hertfordshire, UK). The images were quantified using ImageJ (NIH, USA) software.

Statistical analysis

All data analysis was performed using IBM SPSS Statistics v21 and Prism 5.0 software. The two factor analysis of variance was used with strain (BEH or BEH+/+), treatment (FO or control) as main effects and strain by treatment interaction. A repeated measures design was followed in the analyses of muscle weight (two levels; overloaded and contralateral leg) and fatigue test (twenty levels). A Greenhouse-Geisser correction was applied in the fatigue test data analyses to compensate for the violation of sphericity. All the tests were two tailed with significance level was set at $P < 0.05$.

Results

Data on CS activity in SOL, GAS and PLAN muscles of BEH+/+ and BEH mice at the baseline without FO are presented in Fig. 1. BEH mice showed lower ($P < 0.05$) CS activity than BEH+/+ mice in PLAN and GAS muscles which did not differ in this measurements. The pattern was different for SOL which did not show any difference in CS activity between BEH and BEH+/+ strains. BEH mice had higher CS activity for SOL compared to GAS ($P < 0.01$) and PLAN ($P < 0.001$) though these three muscles did not differ in BEH+/+ strain.

Table 1 contains data on body mass of BEH+/+ and BEH mice in experiments with FO of SOL muscle. BEH mice were heavier ($P < 0.001$) than BEH+/+ mice. Body mass of mice did not change during the period of FO and did not differ from the age matched controls. Data on muscle mass, optimal length, peak isometric force and specific force are presented in Fig. 1. Sol was heavier in BEH mice compared to BEH+/+ mice ($P < 0.001$). FO induced a marked gain in SOL mass ($P < 0.001$). When adjusted for the weight of the contralateral SOL, the relative gain in BEH+/+ strain was greater than in BEH strain (mean ± S.D., 34.9 ± 11.5 % vs 17.7 ± 11.9 %, respectively, $P < 0.01$). These changes of muscle weight reflected greater relative gain in dry muscle mass for BEH+/+ compared to BEH strain (36.1 ± 11.8 % versus 16.0 ± 10.5%, respectively, $P < 0.01$). Muscle mass of the contralateral control SOL did not differ from muscle mass of the age-matched controls that were not subjected to functional overload. There were no differences in optimal muscle length of SOL between BEH and BEH+/+ mice that were not subjected to FO. FO induced an increase in the muscle length ($P < 0.05$) in BEH mice, but not BEH+/+ mice. BEH mice generated greater peak force ($P < 0.01$) compared to BEH+/+ mice in the control condition, but the differences between the strains disappeared after functional overloading; BEH mice showed a decrease in peak isometric force while this parameter did not change in BEH+/+ mice. Thus FO induced a

decrease in specific force in both strains of mice, but specific force was lower in BEH compared to BEH+/+ mice at each time point ($P < 0.001$).

Twitch contractile properties are shown in Fig. 3. BEH mice generated twitches with shorter contraction time ($P < 0.001$) and half relaxation time ($P < 0.001$) compared to BEH+/+ mice. Twitch to tetanus force ratio was also lower in BEH mice compared to BEH+/+ mice. Functional overloading did not have any significant effect on these twitch properties.

Data on changes in p70S6K phosphorylation and cytochrome c are presented in Fig. 4. There were no significant differences between BEH+/+ and BEH mice in these measurements. p70S6K phosphorylation did not change after FO. Cytochrome c to β-Actin ratio tended to be higher in BEH mice compared to BEH+/+ ($P = 0.08$). FO did not induce any change in this ratio.

Data on the peak isometric force during 20 eccentric contractions and CK efflux after the exercise are presented in Fig. 5. Changes in the peak force differed depending on the strain and treatment (strain by treatment by time interaction, $P < 0.001$). The BEH muscles showed a greater drop in the peak force than BEH+/+ muscles ($P < 0.05 – 0.0001$) when studied in the control condition. FO reduced the force loss in BEH muscles to the level of BEH+/+ strain which did not show any changes in the force loss after this intervention. There were no differences between BEH and BEH+/+ in muscle CK efflux after exercise. Muscle CK efflux was not modulated by the adaptation to FO.

Discussion

The main aim of the study was to test the hypothesis that myostatin dysfunction promotes muscle hypertrophy and strength gain in response to FO. We studied the effects of ablation of the gastrocnemius muscle on muscle properties of Sol in BEH and BEH+/+ mice since this

model permitted us to examine the role of myostatin in muscle adaptation to high functional demands. The results reject our original hypothesis, since BEH mice showed smaller rather than greater gain in muscle mass compared to BEH+/+ and exhibited a decrease rather than an increase in peak isometric force after FO. Thus myostatin dysfunction might impair adaptations to increased functional demands in skeletal muscles with high oxidative capacity.

Contractile properties

We studied slow twitch SOL, but our results on baseline muscle properties agree well with findings on fast twitch extensor digitorum longus muscle of BEH mice (Amthor *et al.*, 2007). SOL of BEH mice showed bigger muscle mass, faster twitch speed and reduced specific force compared to BEH+/+ mice. This high twitch speed could be attributed to a shift in muscle fibre composition towards faster contracting myosin isoforms and fibre types in mice with myostatin dysfunction (Amthor *et al.*, 2007, Matsakas *et al.*, 2010). However, the decrease in specific force is not expected from the changes in muscle fibre composition because type 2 fibres often show higher specific force than type 1 fibres (Bottinelli *et al.*, 1996). It appears that effects of myostatin inhibition are not limited to changes in the fibre type composition. SB431542 mediated inhibition of myostatin signaling lead to an increase in cross sectional area with no change in peak isometric force of muscle fibre in Xenopus laevis (Watt *et al.*, 2010). One of the reasons for a decrease in specific force could be due to low levels of contractile proteins in muscle fibres of mice showing myostatin dysfunction (Qaisar *et al.*, 2012). Enlarged myonuclear domains might limit protein synthesis and accumulation of contractile protein in muscle fibres showing excessive hypertrophy (Qaisar *et al.*, 2012). However, this is an oversimplified view since myostatin inhibits protein synthesis and removal of this inhibition is expected to have a positive effect on the overall protein synthesis rates (Goodman *et al.*, 2013). Interestingly, specific muscle force increased in mice with

myostatin knock out after a period of endurance training or food restriction which lead to a decrease in the cross sectional area of skeletal muscles (Matsakas *et al.*, 2012, Matsakas *et al.*, 2013). It has been suggested that accumulation of aberrant p62 proteins might interfere with force generation in muscle fibres of myostatin deficient mice fed ad libitum (Collins-Hooper *et al.*, 2015). Interestingly, BEH and BEH+/+ mice did not differ in specific force of SOL at the age of 31-35 days when muscle mass was less than half of the adult size (Baltusnikas *et al.* in press). It might be that biomechanical factors such as an increase in muscle fibre pennation angles also have a negative effect on force generating capacity of hypertrophied muscles in addition to the factors acting at the single fibre level (Amthor *et al.*, 2007).

Functional overloading (FO)

We used 4 week exposure to FO. It is a popular model to study muscle hypertrophy in mammals (Lowe and Alway, 2002). This type of muscle overloading leads to an increase in muscle mass with less pronounced increase in force generating capacity in mouse PLAN (Bodine and Baar, 2012). A similar force deficit is observed in skeletal muscles of rats (Kandarian and White, 1989). We focused on SOL which can be excised intact for assessment of contractile properties and contains a mixture of muscle fibre types resembling human muscles (Bloemberg and Quadrilatero, 2012). It is expected that the effects of FO and myostatin inhibition would vary between skeletal muscles that differ in muscle fibre type composition and other properties. SOL showed a relatively small increase in muscle mass and no increase in peak isometric force which is in contrast to the previous findings on PLAN after FO (Bodine and Baar, 2012). The majority of studies on the role of myostatin in rodents focused on the muscles dominated by type 2B fibres (Amthor *et al.*, 2007, Matsakas *et al.*, 2010, Matsakas *et al.*, 2012). The observed effects of myostatin on the tibialis anterior and

extensor digitorum muscles are typically large and stimulated the interest in it as a possible pharmacological target (Mendias *et al.*, 2006). However, human muscles are rather different as no 2B fibres are detected (Smerdu and Erzen, 2001). The present study on the role of myostatin indicated that, contrary to expectation, the potential for gain in muscle mass and function might be limited in the muscles comprised of type 1 and type 2A fibres.

A particular feature of adaptation to functional overloading in BEH strain was an increase in optimal muscle length which did not change in BEH+/+ strain. Severe muscle exercise is associated with muscle injury, increased heterogeneity of sarcomere length and increased muscle optimal length (Proske and Morgan, 2001). Functional overloading does induce muscle injury especially during the first week of its application (Lowe and Alway, 2002). It appears that myostatin dysfunction increases muscle susceptibility to injury after exercise (Mendias *et al.*, 2006, Baltusnikas *et al.*, in press). Indeed, SOL of BEH mice showed a faster drop in peak force in repeated eccentric contractions compared to BEH+/+ strain eventhough muscle CK efflux was similiar. Muscle injury and the associated inflammatory response can inhibit accumulation of contractile proteins and lead to a decrease in specific force (Pizza *et al.*, 2002). Inhibition of signalling by transforming growth factor- β (TGF-β) superfamily, which myostatin is a member of, impairs muscle regeneration and leads to a long term deficit in force production after exercise-induced injury ((McPherron *et al*., 1997, Gumucio *et al.*, 2013). SOL shows particularly high involvement in motor activities compared to other limb muscles (Roy *et al.*, 1991). Interestingly, cancer cachexia which is associated with increased serum levels of inflammatory cytokines leads to a decrease in specific force of the diaphragm with high levels of activity, but not in other less active muscles (Roberts *et al.*, 2013). It appears that myostatin dysfunction interferes with in adaptation of SOL to the overloading. There were no changes in mitochondrial cytochrome c levels, and reduction in force loss during eccentric exercise was not due to improved oxidative capacity of muscles in BEH

mice after FO. It is likely that a decrease in specific force might have played an important role in this phenomenon.

Anabolic signaling

BEH and BEH+/+ mice showed similar CS activity and cytochrome c levels in SOL which was in contrast to GAS and PLAN showing reduced CS activity in BEH mice compared to BEH+/+ mice. It appears that myostatin dysfunction has a less marked effect on oxidative capacity of SOL compared to other limb muscles (Collins-Hooper *et al.*, 2015). There was also no difference between SOL of BEH+/+ and BEH mice in P70S6K phosphorylation which has been linked to muscle growth in rats (Baar and Esser, 1999). In contrast to the other limb muscles, rat SOL showed only a small increase in P70S6K phosphorylation immediately after electrical stimulation mimicking high resistance exercise and this change became insignificant within 3 hours of recovery. It appears that mouse SOL also shows a reduced signaling through mTOR - P70S6K axis compared to GAS which has been used to study effects of myostatin knockout (Lipina *et al.*, 2010). Importance of mTOR signaling for muscle growth also varies with time of exposure to the hypertrophic stimuli. P70S6K phosphorylation returns to baseline levels within 21 days of FO in fast twitch PLAN (Hamilton *et al.*, 2014). In general, our results agree with the contention that mTOR signaling is not a predictor of muscle hypertrophy in response to the long term functional overloading.

Perspevtives

Myostatin inhibition has attracted a considerable interest as a strategy for improvement of muscle function. A significant effort has been spent in studying effects of myostatin inhibition on muscle cells and skeletal muscles in various mouse models. Much less attention has been devoted to effects of myostatin dysfunction on the muscle adaptations to various

types of functional overlaoding and muscle exercise. Our results show that BEH mice had expereienced a smaller rather than greater gain in SOL mass and, in contrast to BEH+/+ mice, exhibited a decrease in muscle force generating capacity after functional overloading. These results suggest that myostatin dysfunction has a negative effect on adaptation to increased functional demands in skeletal muscles with high levels of motor activity.

Competing interests

There are no competing interests

Acknowledgments

This project was also supported by Marie Curie International Reintegration Grant 249156 (A. Lionikas) and the grants VP1-3.1-ŠMM-01-V-02-003 (A. Kilikevicius) and MIP-067/2012 (T. Venckunas) from the Research Council of Lithuania. We wish also to thank Mrs Indre Libnickiene for her excellent technical assistance provided during the project.

References

Amthor H, Macharia R, Navarrete R, Schuelke M, Brown SC, Otto A, Voit T, Muntoni F, Vrbova G, Partridge T, Zammit P, Bunger L & Patel K. Lack of myostatin results in excessive muscle growth but impaired force generation. Proc Natl Acad Sci U S A 2007: 104: 1835-1840.

Baar K, Esser K. Phosphorylation of p70(S6k) correlates with increased skeletal muscle mass following resistance exercise. Am J Physiol 1999: 276: C120-C127.

Baltusnikas J, Kilikevicius A, Venckunas T, Fokin A, Lionikas A, Ratkevicius A. Regenerated soleus muscle shows reduced creatine kinase efflux after contractile activity in vitro. Appl Physiol Nutr Metab 2015: 40: 129-133.

Baltusnikas J, Kilikevicius A, Venckunas T, Fokin A, Bünger L, Lionikas A, Ratkevicius A. Myostatin dysfunction impairs force generation in extensor digitorum longus muscle and

increases exercise-induced protein efflux from extensor digitorum longus and soleus muscles. *Appl Physiol Nutr Metab* (In press).

Bloemberg D, Quadrilatero J. Rapid determination of myosin heavy chain expression in rat, mouse, and human skeletal muscle using multicolor immunofluorescence analysis. PLoS One 2012: **7**: e35273, DOI: 10.1371/journal.pone.0035273.

Bodine SC, Baar K (2012). Analysis of skeletal muscle hypertrophy in models of increased loading. Methods Mol Biol 2012: 798: 213-229.

Bogdanovich S, Krag TO, Barton ER, Morris LD, Whittemore LA, Ahima RS, Khurana TS. Functional improvement of dystrophic muscle by myostatin blockade. Nature 2002: 420: 418-421.

Bottinelli R, Canepari M, Pellegrino MA, Reggiani C. Force-velocity properties of human skeletal muscle fibres: myosin heavy chain isoform and temperature dependence. J Physiol 1996: 495 (Pt 2), 573-586.

Brooks SV & Faulkner JA. Contractile properties of skeletal muscles from young, adult and aged mice. *J Physiol* 1988: 404, 71-82.

Bunger L, Ott G, Varga L, Schlote W, Rehfeldt C, Renne U, Williams JL & Hill WG. Marker-assisted introgression of the Compact mutant myostatin allele MstnCmpt-dl1Abc into a mouse line with extreme growth effects on body composition and muscularity. Genet Res 2004: 84, 161-173.

Collins-Hooper H, Sartori R, Giallourou N, Matsakas A, Mitchell R, Mararenkova H, Flasskamp H, Macharia R, Ray S, Swann JR, Sandri M, Patel K. Symmorphosis through Dietary Regulation: A Combinatorial Role for Proteolysis, Autophagy and Protein Synthesis in Normalising Muscle Metabolism and Function of Hypertrophic Mice after Acute Starvation. PLoS One 2015: **10**: e0120524, DOI: 10.1371/journal.pone.0120524.

Goodman CA, Frey JW, Mabrey DM, Jacobs BL, Lincoln HC, You JS, Hornberger TA. The role of skeletal muscle mTOR in the regulation of mechanical load-induced growth. J Physiol 2011: 589: 5485-5501.

Goodman CA, McNally RM, Hoffmann FM, Hornberger TA. Smad3 Induces Atrogin-1, Inhibits mTOR and Protein Synthesis, and Promotes Muscle Atrophy In Vivo. Mol Endocrinol 2013: 27: 1946-1957.

Gumucio JP, Flood MD, Phan AC, Brooks SV, Mendias CL. Targeted inhibition of TGF-β results in an initial improvement but long-term deficit in force production after contraction-induced skeletal muscle injury. J Appl Physiol 2013: 115: 539–545.

Hamilton DL, Philp A, MacKenzie MG, Baar K. A limited role for PI(3,4,5)P3 regulation in controlling skeletal muscle mass in response to resistance exercise. PLoS One 2010: **5**: e11624, DOI: 10.1371/journal.pone.0011624; 10.1371/journal.pone.0011624.

Hamilton DL, Philp A, MacKenzie MG, Patton A, Towler MC, Gallagher IJ, Bodine SC, Baar K. Molecular brakes regulating mTORC1 activation in skeletal muscle following synergist ablation. Am J Physiol Endocrinol Metab 2014: 307: E365-E373.

Jacobs RA, Diaz V, Meinild AK, Gassmann M, Lundby C. The C57Bl/6 mouse serves as a suitable model of human skeletal muscle mitochondrial function. Exp Physiol 2013: DOI: 10.1113/expphysiol.2012.070037.

Kandarian SC, White TP. Force deficit during the onset of muscle hypertrophy. J Appl Physiol 1989: 67: 2600-2607.

Kilikevicius A, Venckunas T, Zelniene R, Carroll AM, Lionikaite S, Ratkevicius A, Lionikas A. Divergent physiological characteristics and responses to endurance training among inbred mouse strains. Scand J Med Sci Sports 2012: 23(5): 657-668.

Lionikas A, Kilikevicius A, Bunger L, Meharg C, Carroll AM, Ratkevicius A, Venckunas T, Blizard DA. Genetic and genomic analyses of musculoskeletal differences between BEH and BEL strains. Physiol Genomics 2013: 45: 940-947.

Lipina C, Kendall H, McPherron AC, Taylor PM, Hundal HS. Mechanisms involved in the enhancement of mammalian target of rapamycin signalling and hypertrophy in skeletal muscle of myostatin-deficient mice. FEBS Lett 2010: 584: 2403-2408.

Lowe DA, Alway SE. Animal models for inducing muscle hypertrophy: are they relevant for clinical applications in humans?. J Orthop Sports Phys Ther 2002: 32, 36-43.

MacKenzie MG, Hamilton DL, Pepin M, Patton A, Baar K. Inhibition of myostatin signaling through Notch activation following acute resistance exercise. PLoS One 2013: 8: e68743, DOI: 10.1371/journal.pone.0068743.

Matsakas A, Macharia R, Otto A, Elashry MI, Mouisel E, Romanello V, Sartori R, Amthor H, Sandri M, Narkar V, Patel K. Exercise training attenuates the hypermuscular phenotype and restores skeletal muscle function in the myostatin null mouse. Exp Physiol 2012*:* 97: 125-140.

Matsakas A, Mouisel E, Amthor H, Patel K. Myostatin knockout mice increase oxidative muscle phenotype as an adaptive response to exercise. J Muscle Res Cell Motil 2010: 31: 111-125.

Matsakas A, Romanello V, Sartori R, Masiero E, Macharia R, Otto A, Elashry M, Sandri M, Patel K. Food restriction reverses the hyper-muscular phenotype and force generation capacity deficit of the myostatin null mouse. Int J Sports Med 2013*:* 34: 223-231.

McPherron AC, Lawler AM, Lee SJ. Regulation of skeletal muscle mass in mice by a new TGF-beta superfamily member. Nature 1997: 387: 83-90.

Mendias CL, Marcin JE, Calerdon DR, Faulkner JA. Contractile properties of EDL and soleus muscles of myostatin-deficient mice. J Appl Physiol 2006: 101, 898-905.

Pizza FX, Koh TJ, McGregor SJ, Brooks SV. Muscle inflammatory cells after passive stretches, isometric contractions, and lengthening contractions. J Appl Physiol 2002*:* 92, 1873-1878.

Proske U, Morgan DL. Muscle damage from eccentric exercise: mechanism, mechanical signs, adaptation and clinical applications. J Physiol *2001:* 537: 333-345.

Qaisar R, Renaud G, Morine K, Barton ER, Sweeney HL, Larsson L. Is functional hypertrophy and specific force coupled with the addition of myonuclei at the single muscle fiber level?. FASEB J 2012: 26: 1077-1085.

Ratkevicius A, Carroll AM, Kilikevicius A, Venckunas T, McDermott KT, Gray SR, Wackerhage H, Lionikas A. H55N polymorphism as a likely cause of variation in citrate synthase activity of mouse skeletal muscle. Physiol Genomics 2010: 42A: 96-102.

Ratkevicius A, Joyson A, Selmer I, Dhanani T, Grierson C, Tommasi AM, DeVries A, Rauchhaus P, Crowther D, Alesci S, Yaworsky P, Gilbert F, Redpath TW, Brady J, Fearon KC, Reid DM, Greig CA, Wackerhage H. Serum concentrations of myostatin and myostatin-interacting proteins do not differ between young and sarcopenic elderly men. J Gerontol A Biol Sci Med Sci 2011: 66: 620-626.

Roberts BM, Frye GS, Ahn B, Ferreira LF, Judge AR. Cancer cachexia decreases specific force and accelerates fatigue in limb muscle. Biochem Biophys Res Commun 2013*:* 435: 488-492.

Roy RR, Hutchison DL, Pierotti DJ, Hodgson JA, Edgerton VR. EMG patterns of rat ankle extensors and flexors during treadmill locomotion and swimming. J Appl Physiol 1991*:* 70, 2522-2529.

Smerdu V, Erzen I. Dynamic nature of fibre-type specific expression of myosin heavy chain transcripts in 14 different human skeletal muscles. J Muscle Res Cell Motil 2001*:* 22, 647-655.

Smith RC & Lin BK (2013). Myostatin inhibitors as therapies for muscle wasting associated with cancer and other disorders. Curr Opin Support Palliat Care 2013: 7: 352-360.

Stewart VH, Saunders DH, Greig CA. Responsiveness of muscle size and strength to physical training in very elderly people: A systematic review. Scand J Med Sci Sports 2013: DOI: 10.1111/sms.12123..

Verdijk LB, Gleeson BG, Jonkers RA, Meijer K, Savelberg HH, Dendale P, van Loon LJ. Skeletal muscle hypertrophy following resistance training is accompanied by a fiber type-specific increase in satellite cell content in elderly men. J Gerontol A Biol Sci Med Sci 2009**:** 64: 332-339.

Watt KI, Jaspers RT, Atherton P, Smith K, Rennie MJ, Ratkevicius A, Wackerhage H. SB431542 treatment promotes the hypertrophy of skeletal muscle fibers but decreases specific force. Muscle Nerve 2010: 41: 624-629.

Table 1. Body mass of experimental BEH+/+ (n=12) and BEH (n=9) mice that were subjected to functional overloading (FO) of soleus muscle and body mass of aged matched +/+ (n=12) and *C*/*C* (n=12) mice that were not subjected to any interventions.

	Experimental mice		Control mice
	Before FO 14 weeks	After FO 18 weeks	18 weeks
BEH+/+ (g)	54.0 ± 3.3	54.1 ± 3.3	52.0 ± 3.6
BEH (g)	61.0 ± 4.0***	60.4 ± 4.4***	60.2± 3.1***

Values are means ± SD *** $P < 0.001$ between BEH+/+ and BEH mice.

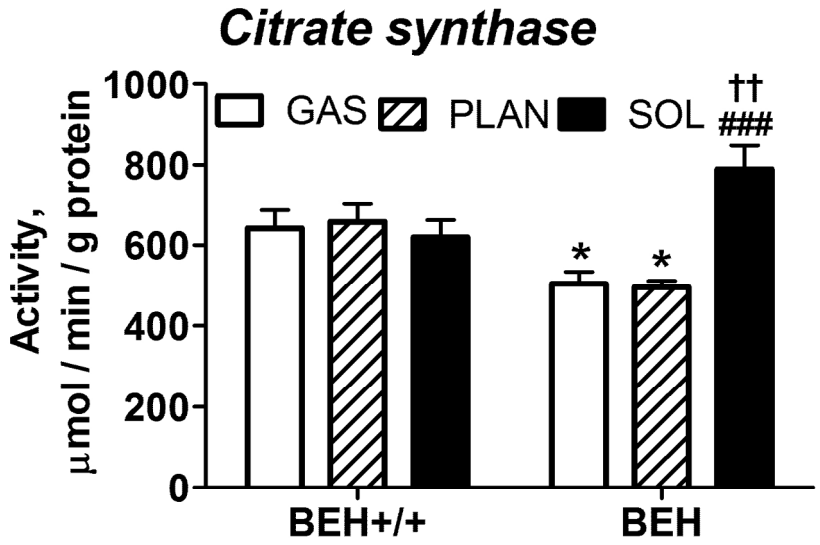

Fig. 1. Citrate synthase (CS) activity in the gastrocnemius (GAS), plantaris (PLAN) and soleus (SOL) muscles of BEH+/+ (n=6) and BEH (n=6) mice. Values are means ± SEM; * $p < 0.05$ versus BEH+/+ mice; †† $P < 0.01$ versus Gas of BEH mice; ### $P < 0.001$ versus Plan of BEH mice.
170x104mm (300 x 300 DPI)

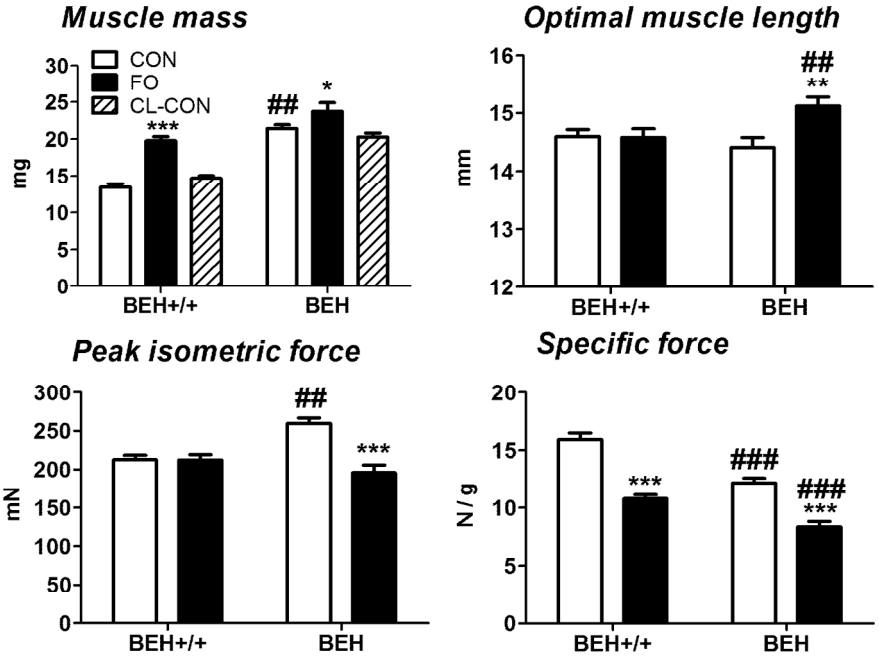

Fig. 2. Muscle mass, optimal length, peak isometric force and specific force of soleus muscles (SOL) in the control condition without any intervention (CON) and after 28 days of functional overloading (FO) with the respective contralateral controls (CL-CON) where appropriate for BEH+/+ (n=12) and BEH (n=9) mice. Values are means ± SEM; * P < 0.05, *** P < 0.001 between control and functional overload (FO) muscles; ## P < 0.01, ### P < 0.001 between BEH+/+ and BEH muscles.
169x121mm (300 x 300 DPI)

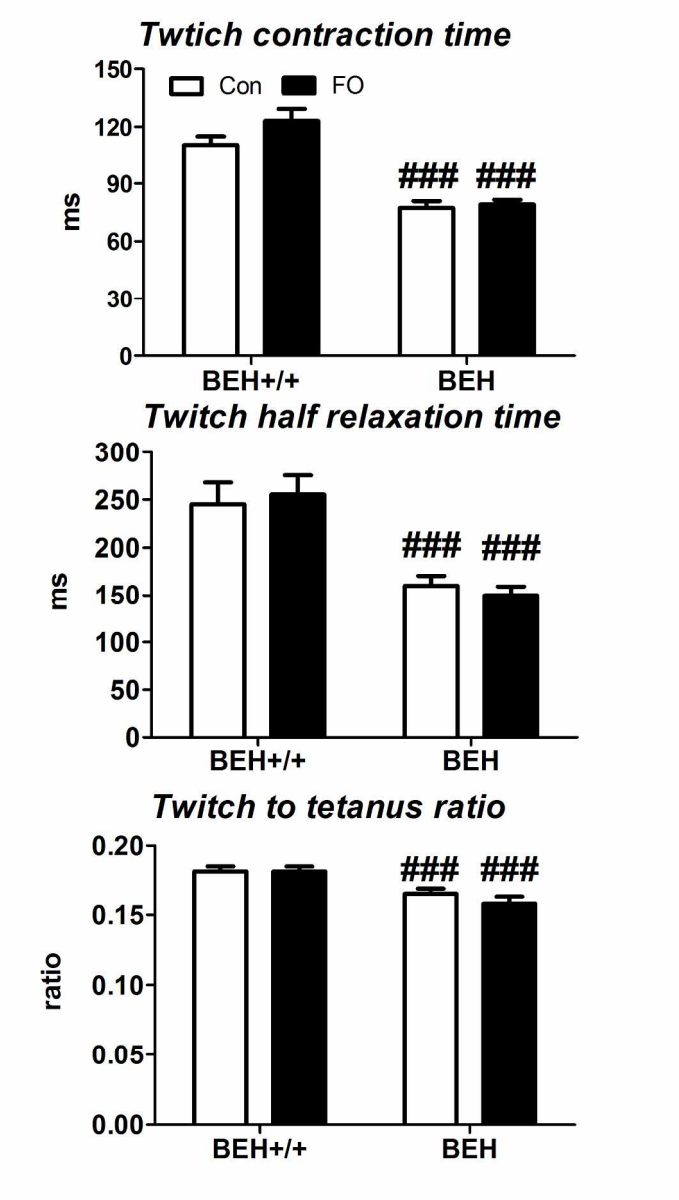

Fig. 3. Twitch contractile properties of soleus muscle (SOL) in the control (CON) BEH+/+ (n=12) and BEH (n=12) mice and after 28 days of functional overloading (FO) for BEH+/+ (n=12) and BEH (n=9) mice. Values are means ± SEM; ### P < 0.001 between BEH+/+ and BEH muscles.
145x257mm (300 x 300 DPI)

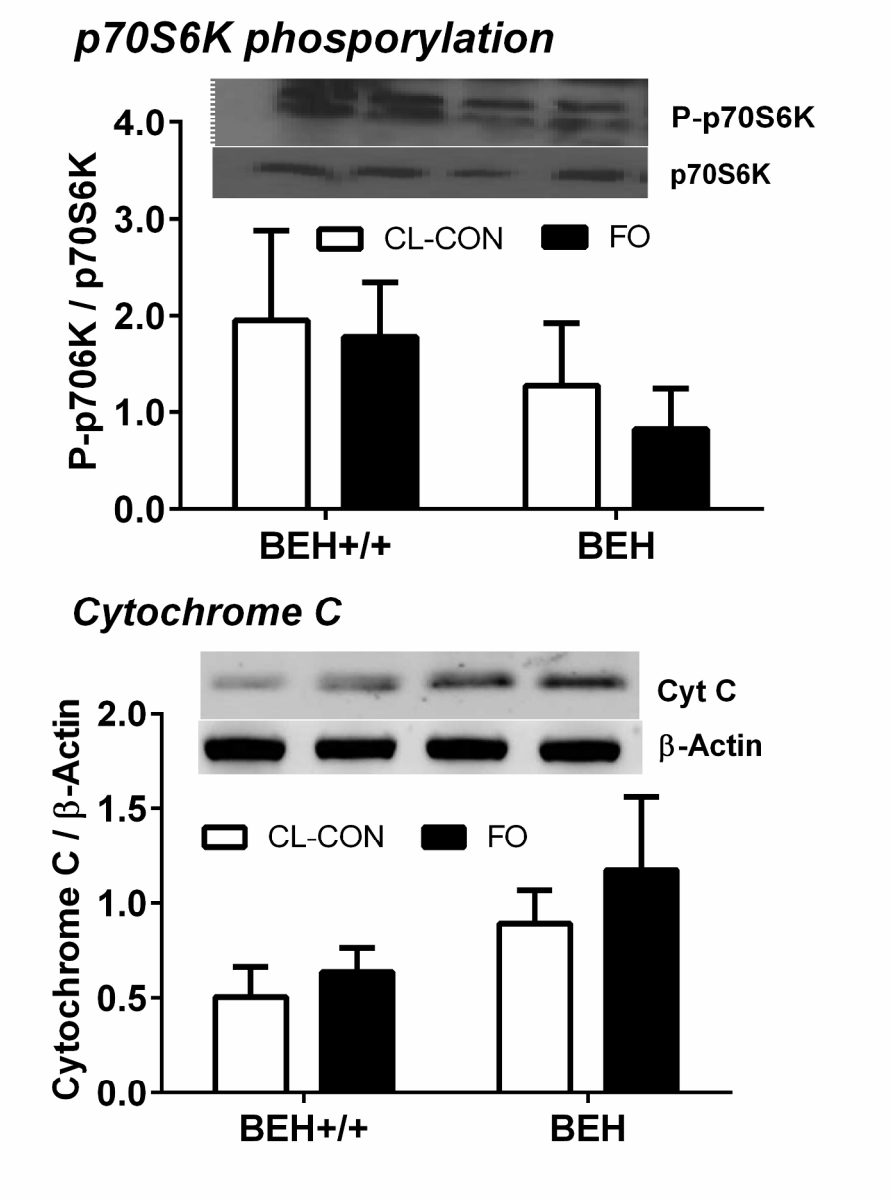

Fig. 4. p70S6K phosphorylation (P-p70S6K/p70S6K ratio) and cytochorome c (Cyt C) in the soleus muscle (SOL). Western bloting was performed on the contralateral control (CL-CON) muscles and the muscle after 28 days of functional overloading (FO) for BEH+/+ (n=6) and BEH (n=6) mice. The representative Western blots are shown for each of the four studied muscle groups in the same order as bars in the figure. Values are means ± SEM.
206x277mm (300 x 300 DPI)

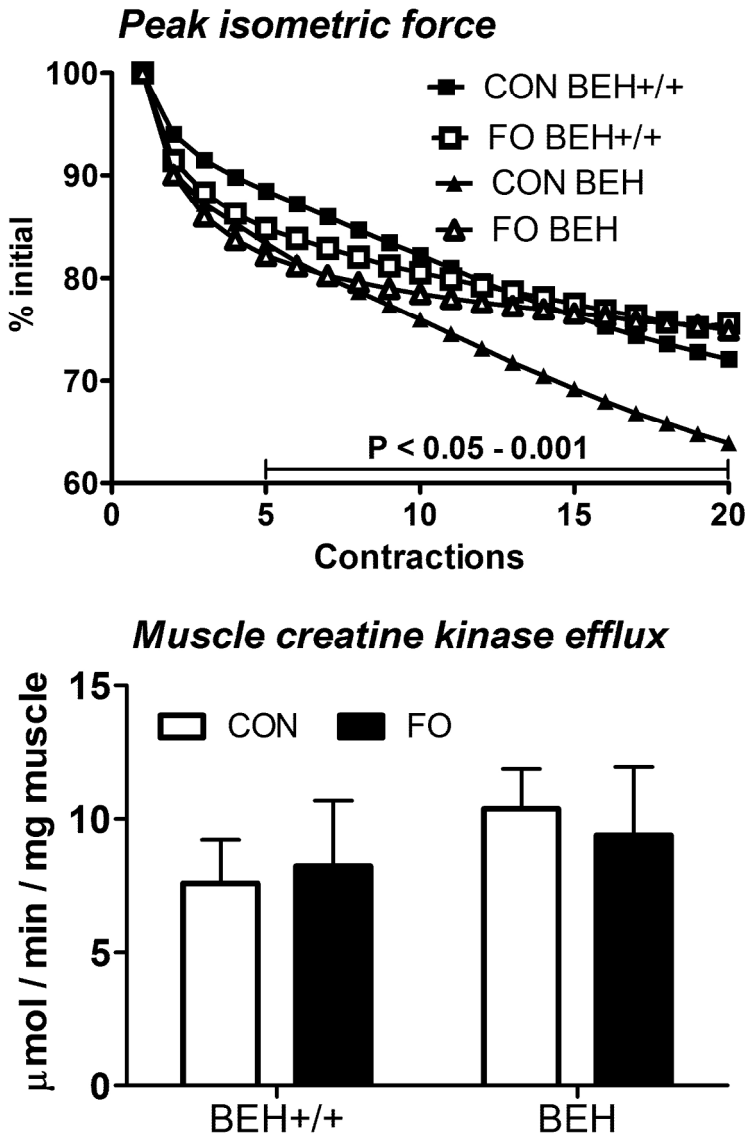

Fig. 5. Peak isometric force in eccentric exercise and the exercise induced creatine kinase efflux for soleus muscle (SOL) in the control (CON) BEH+/+ (n=12) and BEH (n=12) mice as well as after 28 days of functional overloading (FO) for BEH+/+ (n=12) and BE (n=9) mice, respectively. Values are means ± SEM. As indicated for the control condition, the difference between BEH+/+ and BEH ranged from P < 0.05 after 5 contractions to P < 0.0001 after 20 contractions.
193x257mm (300 x 300 DPI)